Seismic Station Installations and Their Impact on the Recorded Signals and Derived Quantities

Published Version:
castellaro s., alessandrini g., musinu g. (2022). Seismic Station Installations and Their Impact on the Recorded Signals and Derived Quantities. SEISMOLOGICAL RESEARCH LETTERS, 93(6), 3348-3362 [10.1785/0220220029].

Availability:
This version is available at: https://hdl.handle.net/11585/904014 since: 2022-11-18

Published:
DOI: http://doi.org/10.1785/0220220029

Seismic Station Installations
and their Impact on the Recorded Signals and Derived Quantities

Silvia Castellaro[1*], Giulia Alessandrini[1], Giuseppe Musinu[2]

[1] Dipartimento di Fisica e Astronomia, Alma Mater Studiorum Università di Bologna, viale C. B. Pichat 8, 40127 Bologna, Italy. *Corresponding Author: silvia.castellaro@unibo.it

[2] ENSER srl, viale A. Baccarini 29, Faenza, Ravenna – Italy

Abstract

The role of local geology in controlling ground motion has long been acknowledged. Consequently, increasing attention is paid to the assessment of the geophysical properties of the soils at the seismic stations, which impact the station recordings and a series of related quantities, particularly those referring to seismic hazard estimates. Not the same level of attention is commonly dedicated to the seismic station installation, to the point that it is generally believed that housings/shelters containing seismic instruments are of no interest because they can only affect frequencies well above the engineering range of interest. By using examples from seismometric and accelerometric stations, we describe the 1) housing, 2) foundation and 3) pillar effects on the seismic records. We propose a simple working scheme to identify the existence of potential installation-related issues and to assess the frequency fidelity range of response of a seismic station to ground motion. Our scheme is developed mostly on ambient noise recordings and, thus, surface waves. The hope is that, besides the parameters (Vs30, soil classes etc.) that start to be routinely introduced in the seismic archives, the assessment of the maximum reliable frequency, under which no soil-structure interaction is expected, also becomes a mandatory information. In our experience, for some installation sites, the maximum reliable frequency can even be less than a very few Hz.

Introduction

At the early stages of seismology, seismic stations were installed on stiff rock (Bormann, 2002), to minimize the effects of the fine sediments/rock weathering on the recorded seismic waves. The size of permanent installation seismometers, their need for screws, levelling, batteries and cables led to place them on artificial ground, such as *ad hoc* concrete slabs. There is also sometimes the improper perception that something stiff as a concrete slab or pillar between the sensor and the object of measurement improves the coupling between the two. In addition, to ensure protection from environmental conditions and vandalism, many seismic stations were placed inside small or large structures.

The need for homogenous and dense seismic networks and the increasing interest for the seismic site response and 'local effects' assessment, progressively required seismic stations to be installed on any type of geological condition. In parallel, growingg attention started to be paid to the characterization of the geophysical properties of the soils at the seismic stations (see Cultrera et al., 2021, for a review). In fact, their impact on the station recordings and on the subsequent hazard estimates can be large. On the opposite, not enough attention is still paid to the seismic station installation. It is generally recognized that this can affect the seismic recordings, but it is usually believed that housings/shelters can affect only frequencies well above the engineering range of interest. This led to the habit of naming 'free-field stations', stations that are not under free-field conditions (see also Hollender *et al.,* 2020, who noted the same issues).

The seismic sensor installation can affect seismometer recordings, both under microtremor and earthquake excitation, essentially in 3 strongly interconnected ways that we will discuss in the paper:

1) *Housing effect*: the structure/cabin inside which the sensor is installed has its own dynamics, ruled by its vibration modes. This motion is transmitted to the ground and recorded by the seismometer, even when the latter is placed on a pillar isolated from the foundation by means of a cut all around (Figure 1).
2) *Foundation effect*: stiff foundations (e.g., concrete slab on soft soils) perturb the incident wavefield. Typically, the horizontal motion recorded on the top of a foundation is strongly modified, compared to the free-field motion, at all the wavelengths smaller than and comparable to the foundation size.
3) *Pillar effect*: sensors are often placed on concrete pillars, detached from the foundation by means of a cut, with the intention of dynamically isolating the sensor from the surrounding foundation/structure. We will show that the proximity of the pillar to the foundation and the connection between the two provided by the ground, does not warrant the desired effect.

The effect of foundations on seismic motion was studied by several authors (e.g., Bycroft, 1980; Crouse and Husmand, 1989; Luco *et al.*, 1986; 1990; Castellaro and Mulargia, 2009; Hollender *et al.*, 2020; Cavalieri *et al.*, 2021). Luco *et al.* (1990), as an example, studied 12 different foundation geometries and performed a parametric study, by changing the size, the embedment depth, the extension above the surface. These results, however, strongly depended on the specific input used to study the phenomenon and the conclusions, though very relevant, were difficult to be used because they lacked generality.
As the result of an analysis conducted on earthquake recordings of 5 accelerometric French stations, Hollender et al. (2020) reported a general amplification at high-frequency (> 10 Hz).

On the opposite, focusing on surface waves, Bycroft (1978, 1980) recommended the use of large and thick foundations on nuclear power plants to reduce the seismic input to the overlying structures. If this reduction is clearly welcome in the case of structures to protect them from seismic inputs, it is definitely unwelcome in the case of seismic stations, which are expected to faithfully record the incoming signal (at points 1 or 3 in Figure 1) and not its downsized version on the top of the foundation (point 2 in Figure 1).

The soil-structure interaction and the soil-city interaction were studied by even more authors (*Soil-structure:* Jennings, 1970; Wong and Trifunac, 1975; Bycroft, 1978; Safak, 1998; Guéguen *et al.*, 2000; Chavez-Garcia and Cardenas-Soto, 2002;; Mucciarelli *et al.*, 2003; Cornou *et al.*, 2004;; Guéguen and Bard, 2005;; Ditommaso *et al.*, 2010a,b; Laurenzano *et al.*, 2010; Massa *et al.*, 2010; Castellaro and Mulargia, 2011; Castellaro *et al.*, 2013;; Hollender *et al.,* 2020. *Soil-city:* Wirgin and Bard, 1996; Cloteau and Aubry, 2001; Guéguen *et al.*, 2002; Kham *et al.*, 2006; Schwan *et al.*, 2016; Isbiliroglu *et al.*, 2015; Kumar and Narayan, 2018).

All these studies had little impact on the practical procedures behind seismic installations, also because their effect is hard to predict and to remove.

A recent trend is to move seismometers inside dedicated small fiber-glass cabins (e.g., CER panel in Figure 2): the smaller the foundations, the smaller the range of wavelengths affected by the foundation itself. The smaller the protection structure, the larger its eigen-frequencies (thus beyond the frequency range of engineering interest). However, small fiber-glass structures have much lower stiffness k and mass m compared to traditional structures and since the eigen-frequency of a structure is proportional to $\sqrt{\frac{k}{m}}$, these values can still fall inside the frequency range of engineering interest, altering the motion recorded by the seismometer.

In this paper we provide some examples about: a) the elements that can affect the seismic station fidelity to ground motion, b) how to experimentally assess such fidelity.

Considering the variety of seismic installations that depends on national procedures, on specific soil conditions, on local construction habits, on seismic instrumentation and so on, we do not attempt any systematic/parametric study, but we illustrate the problems by using real examples from seismic stations belonging to the Italian National Seismic or Accelerometric (strong motion, IT) networks.

We use mostly ambient noise recordings, which are dominated by surface waves. Thus, we note since now that our conclusions can differ from those achieved numerically or experimentally by other authors (e.g., Luco *et al.*, 1990; Hollender *et al.*, 2020) who used mostly earthquake recordings. However, as we are going to discuss, we all find that seismic records are severely altered by the soil-station interaction at mid-to-high frequencies.

We concentrate on ambient noise recordings because these types of data are increasingly used in passive seismic applications (seismic noise models, seismic site amplification assessments with ambient noise, etc.) and because ambient noise can be recorded continuously. This allows to obtain average values with narrow standard deviation, which is often not the case when one can work only with few and very different earthquakes (in terms of size, depth, directivity, duration etc.).

We focus on a few stations only, but the potential diffusion of the problem will be discussed at the end of the paper and, as noted by Hollender *et al.* (2020), it is not confined to single nations.

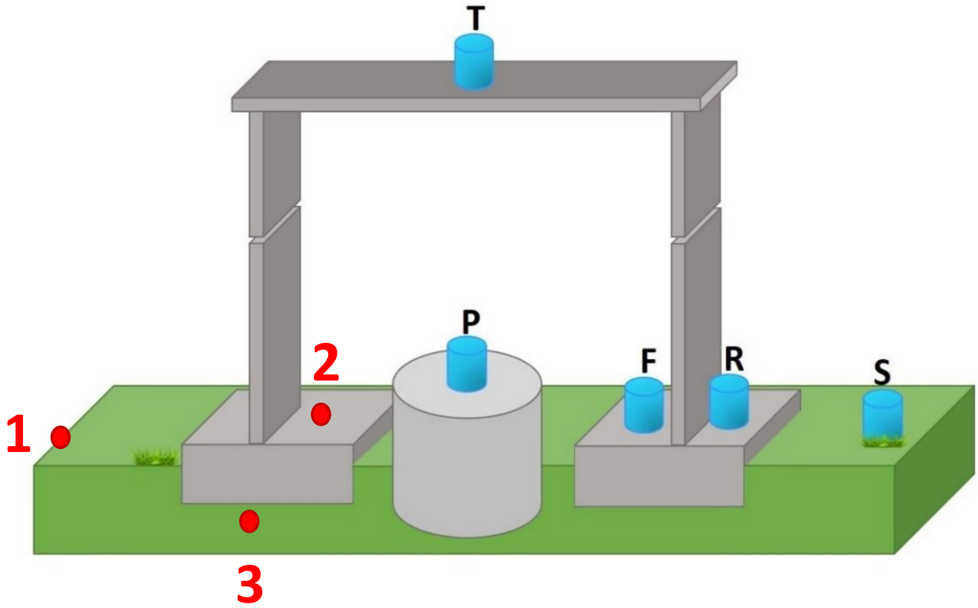

Figure 1. Schematic illustration of a typical seismic installation inside a small structure with a direct foundation. T (top) is the measurement point on the top of the structure (to characterize its fundamental mode), P on the pillar, F on the foundation, R on the foundation rim and S on natural soil.

Elements that can affect the seismic station fidelity to ground motion

We refer to typical seismic stations settled inside big or small structures (Figure 1) and discuss the 1) housing, 2) foundation and 3) pillar impact. These are strongly interconnected, therefore sometimes the discussion will necessarily mix them up.

We use examples from the Italian seismic/accelerometric stations illustrated in Figure 2. For each example we provide the station code, a picture and the soil type synthesized by means of its Vs30. Additional information about each station can be found by searching the station code in the INGV ItAcA database (D'Amico *et al.*, 2020). At the example sites, we collected simultaneous ambient noise measurements at the T (top), P (pillar), F (foundation), R (foundation rim), S (natural soil) locations given in Figure 1.

For all measurements we used Tromino® Blu 3-component portable velocity/acceleration sensors by MoHo srl (Italy), after checking that their response was identical. These instruments have a self-noise lower than $10^{-9} - 10^{-10}$ m/s at the frequencies of interest in this study (> 3 Hz) and were set to have a resolution of $6 * 10^{-11}$ m/s in the ± 0.5 mm/s range. The signal was acquired at all sites for a minimum of 30 minutes, then split into non overlapping window. The FFT was applied to each window and the resulting spectra were smoothed with triangular functions having a width equal to 3 per cent of the central frequency. In the end, the average spectra and their standard deviations were computed.

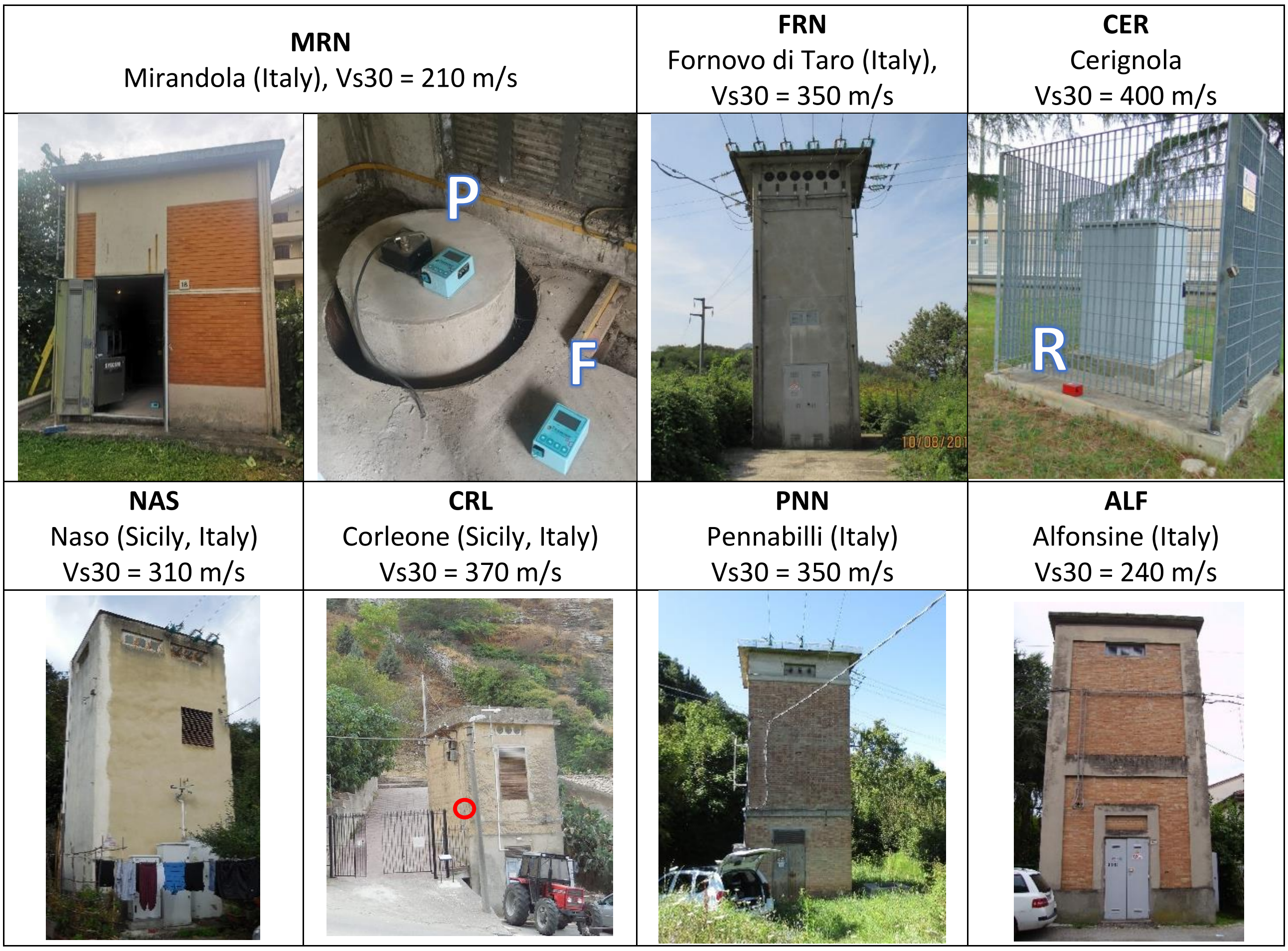

Figure 2. A set of stations of the Italian accelerometric (IT) and seismic (IV) network: small housing (MRN), tower-structures of the national electric service (FRN, NAS, CRL, PNN, ALF) and fiber-glass cabin (CER). A typical pillar with the cut separating it from the foundation is also shown for the MRN station. The pillar is present in most of the Italian installations and can also be square in shape, as in the case of CER. The instruments used for this survey can be seen in the panel of MRN and CER (blue and red boxes). The letter P stands for pillar, F for foundation, R for foundation rim.

The housing effect

Phenomenological evidence

The influence of buildings on ground motion recorded by sensors inside or in their proximity is widely acknowledged (see references in the Introduction). Less acknowledged is the direct influence of the housing on the seismometer recordings that it should protect.

The motion of structures is ruled by the superposition of the motions occurring at their natural frequencies, $f_{i=0,\dots,n}^{Stru}$. When a structure vibrates – due to earthquakes, microtremor, wind – part of this vibration is radiated to the soil and dissipated. The fraction of motion radiated back to the foundation can roughly be estimated by measuring the spectral amplitude of motion on the top of the structure (T in Figure 1) and on its foundation (F or R in Figure 1) or just off the foundation (S in Figure 1), at the same frequencies f_i^{Stru} and time. In practice, this fraction of motion is recorded also by the sensors placed on the pillar (P in Figure 1) because the vibration is efficiently transmitted through the ground.

To show this, we compare the spectra of the motion recorded on the top of the cabins with those recorded at the same time on the pillar or foundation (T/P and T/F ratios) and just outside the cabin (T/S ratios). We also compare the motion recorded on the pillar or foundation with the motion recorded in free-field (P/S, F/S ratios). When no effect is present, we expect these last two ratios to be equal to 1 at all frequencies.

We start from the case of the MRN station, which is hosted in a small cabin (6pprox.. 4 m x 3 m x 4 m, Figure 2), whose modal frequencies are 10 Hz (bending in the transversal direction) and 17 Hz (torsion, better visible in the measurement taken on the perimeter of the roof and clearly less in the proximity of the shear centre), as evident in the T/S_{ref} and T/F spectral ratios of Figure 3. We focus on the transversal direction because it is associated to the lowest resonance frequency, but the same discussion would apply to the longitudinal direction, along which the first bending mode is 15 Hz. We see that the F/S_{ref} and P/S_{ref} spectral ratios are identical, which means that the pillar sensor measures the same things as the foundation sensor, despite the cut all around it. This was observed also in Mucciarelli *et al.* (2003) and Castellaro and Mulargia (2009).

The F/S_{ref} ratio illustrates the role of the foundation on the incoming waves in respect to the real free-field condition. If the foundation had no effect, this ratio should be equal 1 at all frequencies, which is not. S_1/S_{ref} is the ratio between the recording acquired on the soil just off the station (S_1) and on the soil at a few meters distance from the station (usually less than 5 m, S_{ref}). This ratio tends to 1 but there are still some minor differences due to the foundation still very close to S_1.

We note that if the pillar were isolated from the surrounding structure, we should not see any amplification in the P/S_{ref} spectra at the resonance frequencies of the structure. Figure 3 shows that this is not the case: the pillar is affected by the vibration modes of the overlying cabin, in the same way in which the foundation is (F/S_{ref}).

Despite the limited size of the hosting structure, we can assess, from the F/S_{ref} and P/S_{ref} ratios, that the motion recorded from this station is perturbed at frequencies larger than 8 Hz. The torsional mode (17 Hz) is not well acknowledgeable in the foundation measurements due to the foundation effect that we will discuss later in the text.

As a further example, we present in Figure 4 the spectral ratios recorded on the foundation vs. natural soil at two other larger-in-size stations (NAS and PNN, Figure 2). Again, we see that the seismic motion recorded at these sites is perturbed by the eigen-frequencies of the cabin at $\simeq$7 Hz in one case and $\simeq$5 Hz in the other case. These are frequencies of large engineering interest, but the motion recorded from the seismometers at these sites is not a faithful reproduction of the seismic input above ≃6.5 and 4 Hz, respectively.

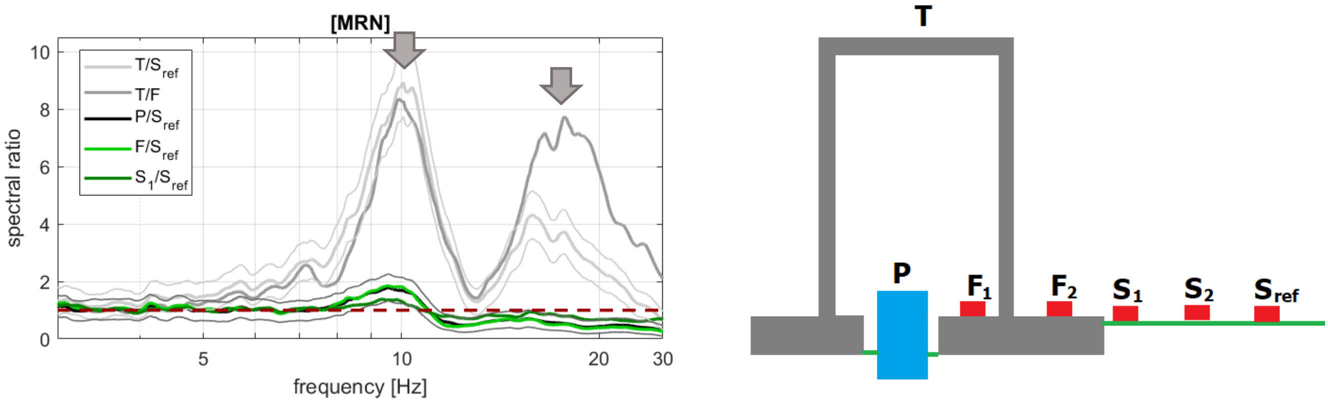

Figure 3. Spectral ratios of the motion recorded along the transversal direction of the cabin MRN at different locations, whose symbols are given in the right panel. The T/S_{ref} and T/F spectral ratios show the natural vibration modes of the structure (gray arrows at 10 Hz mark the trasnvsersal bending mode, at 17 Hz a torsional mode). The P/S_{ref} and F/S_{ref} ratios show the effect of the foundation on the incoming waves in respect to the real free-field condition. If the foundation induced no effect, these ratios should be equal 1 at all frequencies. S_1/S_{ref} is the ratio between the recording acquired on the soil just off the station (S_1) and on the soil at a few meters distance from the station (usually 3-5 m from the foundation rim). S_1/S_{ref} tends to 1 but the eigen-mode of the structure is still visible. The standard deviation of the spectral ratios is shown only in the two extreme cases, not to impair the readability of the plots. It was checked that its amplitude is in the same order of magnitude also when not shown.

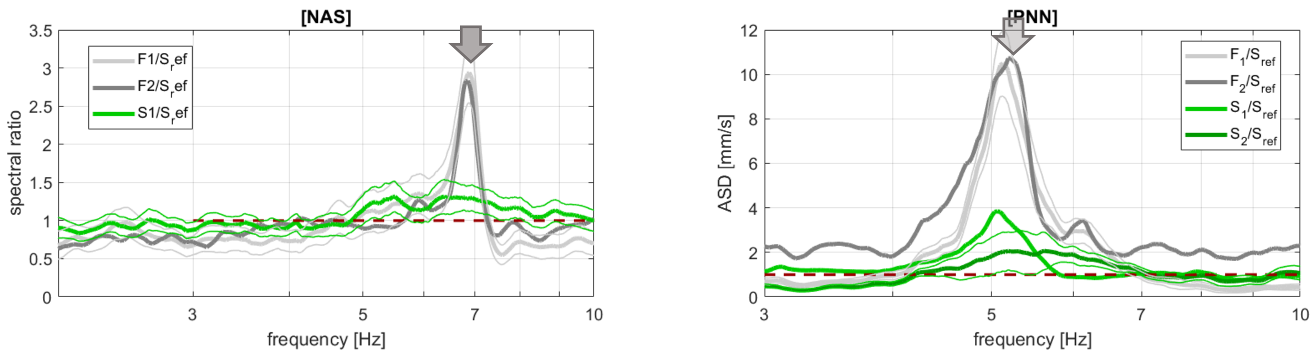

Figure 4. Spectral ratios of the motion recorded along the transversal direction of the cabins NAS and PNN at different locations, whose symbols are given in the right panel of Figure 3. In the F/S_{ref} ratios the natural vibration modes of the structure (6.8 Hz and 5.2 Hz for NAS and PNN, respectively) can be clearly identified. These are progressively less noticeable in the S_1/S_{ref} and S_2/S_{ref} ratios. Thick lines are the average values, thin lines indicate the standard deviations.

Effects on derived quantities

On H/V

Let us now consider the case of CRL station in Sicily (Figure 2). The H/V curve computed from the data recorded by the official instrument installed on the pillar and provided by the national seismic agency is shown on the left panel of Figure 5. It exhibits two peaks passing the SESAME (2004) criteria. In the official station report, the 0.28 Hz frequency peak is indicated as fundamental mode of the site, while the 6 Hz frequency peak is marked as an additional site frequency and it passes even more SESAME (2004) criteria than the fundamental peak.

At this site we performed some measurements inside the niche in the wall of the cabin (red circle in Figure 1) and on the perimeter of the foundation, on natural soil. The spectra of these measurements (right panel in Figure 5) clearly show that the natural modes of the cabin are 7, 18, 30 Hz and are not visible in the free-field S recording, with the only exception of the small disturbance in the vertical component at the fundamental frequency of the structure (7 Hz), which is an effect of structural rocking. This typically has an amplitude which is 1/10 of the horizontal component amplitude.

The 6 Hz H/V peak frequency, identified in the official station report as ‘reliable’, is thus not a soil property but the vibration mode of the cabin, as recorded by the pillar sensor. As a consequence, automatic peak recognition algorithms in the case of sensors installed inside structures of any type should be avoided.

We take this opportunity to note that, despite its large use even on structures, the H/V method (here providing a peak at 6 Hz) is not suitable to detect the resonance of structures (in this case 7 Hz). By dividing the horizontal and vertical components, the H/V ratio mixes different structural behaviors, acting in different directions and occurring at different frequencies. This easily result in a biased estimate of the structure eigenfrequencies, as in this case.

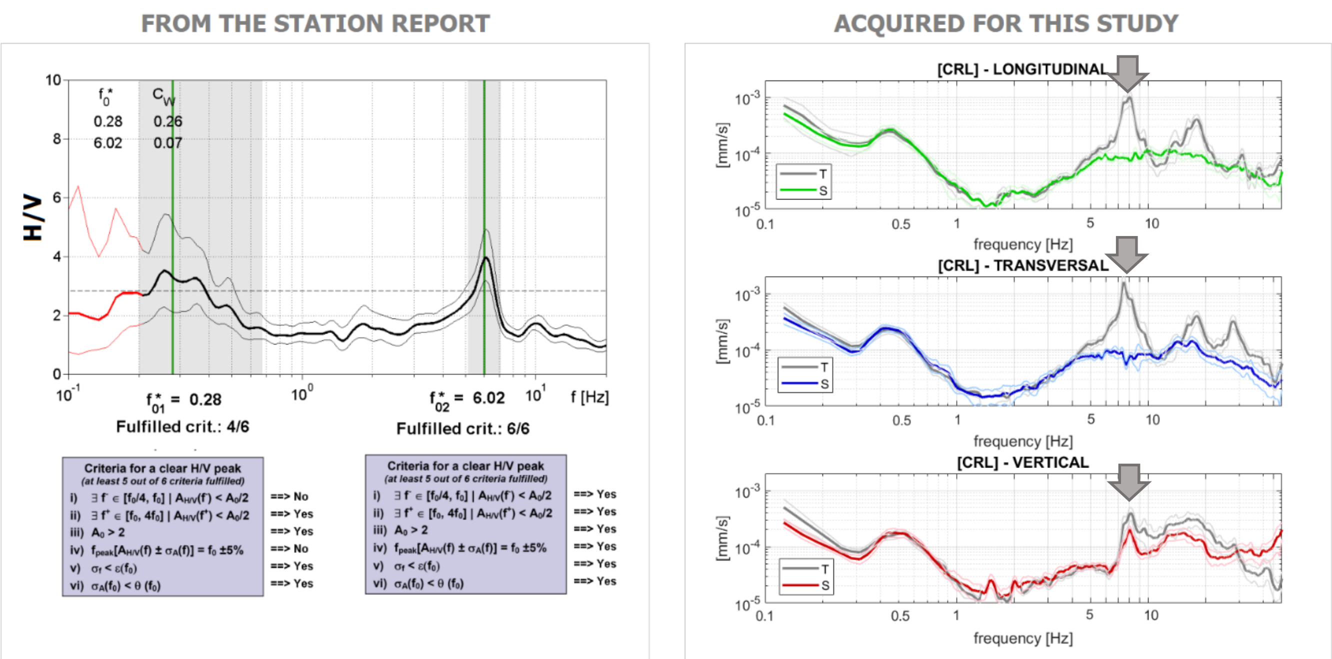

Figure 5. Left panel: H/V curve computed on the data acquired from the official instrument installed on the pillar at the CRL station. According to the station report, 2 peaks pass the SESAME (2004) criteria. Our measurements (right panel), performed on the top of the cabin (T) and on the natural soil just off the station (S) clearly show that the 6 Hz peak is the eigen-period of the cabin and not a soil property. Thick lines are the average values, thin lines indicate the standard deviations.

On response spectra

Let us now consider 10 intermediate size events (scaled to PGA = 0.25 g) recorded in real free-field conditions (black curves in Figure 6) at the MRN site. We treat the MRN housing as single degree of freedom oscillator with natural frequency and damping as directly measured (10 Hz for the transversal component, Figure 3, and 5% damping as computed by the DECÒ method in Castellaro, 2016a). We ignore higher modes because they fall at frequencies of poor engineering interest. Alternatively, they could be considered by mode superposition. We compute the acceleration time series expected on the top of the cabin for the selected input earthquake (red curves in Figure 6a) by means of the Newmark integration approach (e.g., in Clough and Penzien, 1975).

From the T/P ratio in Figure 3 we know the fraction of the cabin motion transmitted to the pillar at all frequencies (e.g., 1/8 for the fundamental frequency), at least under ambient noise excitation. We can thus estimate the free-field motion that would be recorded by the seismometer on the pillar (cyan lines in Figure 6b). This calculation might be not conservative, in the sense that under non-linear behavior it can underestimate the real impact.

We now compute the response spectra of the same input earthquakes as they would be computed from the pillar recording and from the free-field recording, and compare them in Figure 6c. The response spectra calculated from the signals collected on the pillar, P, are much larger than the response spectra computed from the free-field signals (S) at periods close to the natural periods of the housing.

In Figure 6d, e, f we show the same procedure applied to the FRN station (Figure 2). Since the FRN housing eigen-frequencies are lower than the MRN ones (5 Hz vs 10 Hz), the effect on the response spectrum is expected at larger periods, as it is in panel f.

Beyond the hypotheses and assumptions, these examples show that the response spectra computed from a recording performed on a pillar influenced by the surrounding structure can be severely affected at periods close to the structure eigen-period. PGA is also affected but to a minor extent (cyan, P, vs black, S, curves in Figure 6b, e).

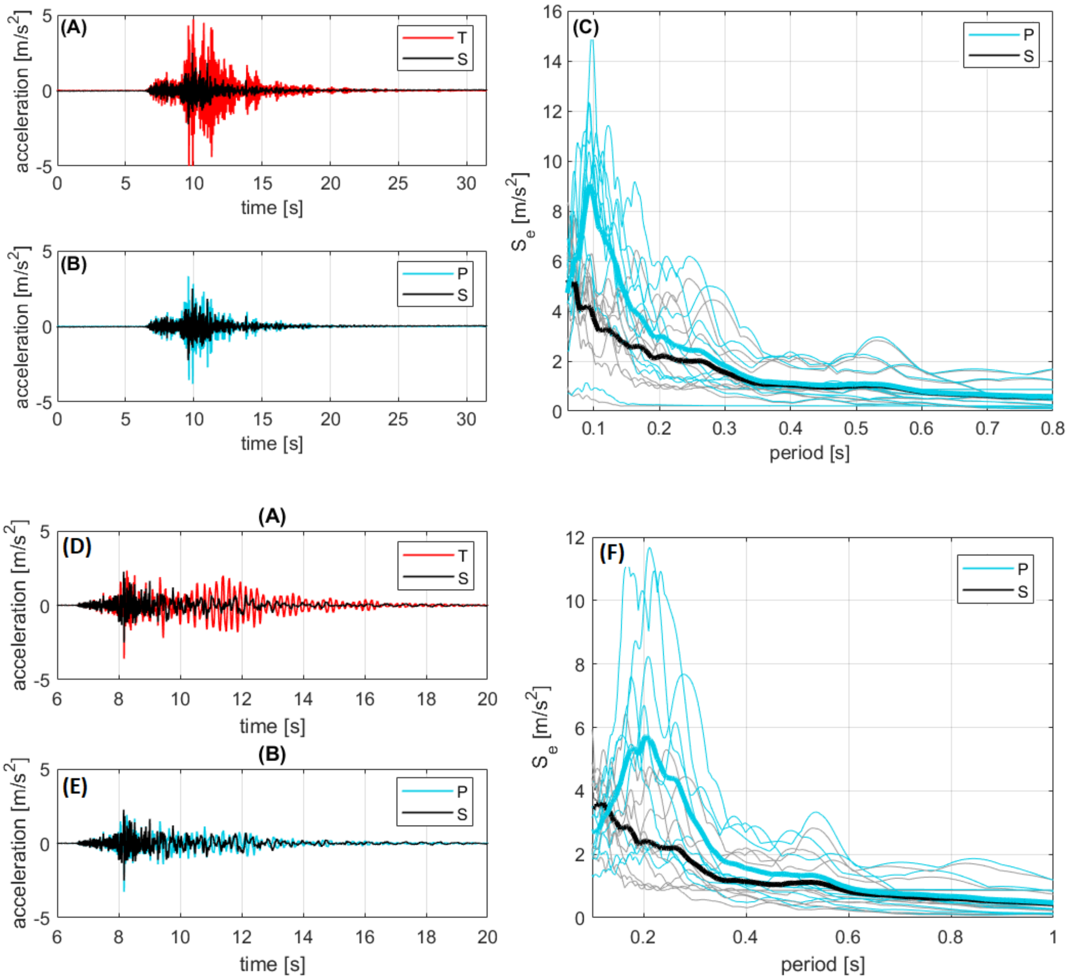

Figure 6. Free-field earthquake records and response spectra (S, black) compared to those recorded on the top of a seismic station (T, red) and on the pillar inside the station (P, cyan). Panels a, b, c refers to the MRN station. Panels d, e, f to the FRN one. The average response spectra (thick lines) are obtained from 10 earthquakes (thin lines). Panels a, b, d, e show just one of the 10 selected earthquakes for each station, as an example.

The results above come from models as no earthquake recordings were available on the top of the station, on the pillar and on the surrounding real free-field conditions at the same time. However, to reproduce these findings with real data, we used ambient noise recordings acquired simultaneously on the pillar and on the garden surrounding the MRN station. The recordings lasted 30 minutes, to obtain a representative average spectrum. As it can be seen in Figure 7, the response spectrum computed from the ambient noise recording acquired on the pillar (cyan) shows the resonance modes of the cabin at 0.06 and 0.1 s (16 and 10 Hz) as dominant peaks, while this is not the case for the response spectrum from ambient noise acquired on the garden surrounding the structure. The two response spectra, in general, are very different.

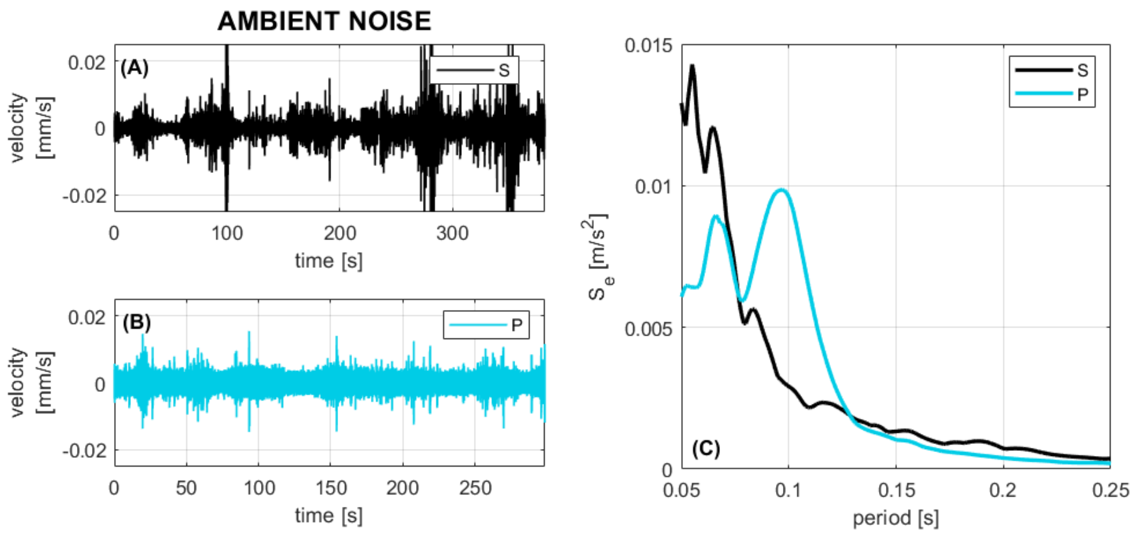

Figure 7. Ambient noise recording acquired in (A) free-field conditions, (B) on the station pillar and response spectra in the two cases (C) for the MRN station. The input signal was 30 min long. Panel (A) an (B) show just a portion of it.

The foundation effect

General issues

After the initial installations on rock, in more recent times seismic stations started to be installed on soft sedimentary covers, both to improve the spatial coverage of seismic networks as well as to capture the so-called seismic site effects (stratigraphic amplification, resonances, etc.). However, the standards of seismic installations (concrete slabs or pillars inside the foundations of hosting structures), did not vary with the underground geology and seismic stations keep on being installed following the original principles.

When an interface has to be placed between the object to measure and the measurement device, the impedance between the interface and the object to measure must be as close as possible, to avoid modifications of the signal due to the interface. This is well acknowledged in the down-hole and cross-hole seismic testing, where, according to ASTM D7400/D7400M-19, the plastic hole casing must be coupled to the ground by using a filling material with seismic impedance as close as possible to the ground itself. On the opposite, this seems to be completely disregarded in seismic station installations. However, while a concrete slab over stiff rocks is theoretically not expected to perturb seismic waves in a significant way, being the rock-to-concrete transition virtually continuous, a concrete slab on soft sediments is expected to perturb seismic waves significantly.

Foundations can be thought as stiff artificial layers that, when overlying softer ones, configure a 'velocity inversion'. This effect on microtremors was largely discussed in Castellaro and Mulargia (2009). They showed both empirically and analytically that whenever a stiffer layer overlies softer ones, the spectra recorded on the stiff layer show deamplified horizontal components compared to the case with no velocity inversion. The vertical component is generally less affected, to the point that a velocity inversion is typically marked by H/V ratios persistently lower than 1.

When a seismic wave hits a stiffer interface, the reflection coefficient is larger than the transmission coefficient (Zoeppritz, 1919). With reference to the red dots in Figure 1 it is generally expected that:

1) incoming surface waves hitting the foundation are reflected backwards and only a fraction of the incoming waves propagate through the medium, from point 1 to 3,
2) body waves travelling from the bottom to the surface are identically reflected downwards and only a fraction of the incoming wave propagates from point 2 to 3,
3) the foundation generates a velocity inversion, which inhibits the existence of the fundamental mode of Love waves (Castellaro, 2016b).

The waves affected by the aforementioned phenomena are, dominantly, those with wavelengths λ comparable to or smaller than the twice the foundation dimensions (for example, a foundation of 5 m size on a clayey soil with $V_S \simeq 150$ m/s will affect approximately the frequencies $f \geq 15$ Hz, see Figure 10). We warn, however, that the real effect is more complex, particularly in the case of earthquake input, as discussed in the Introduction (see also Luco *et al.*, 1990; Hollender *et al.*, 2020).

A decay in the horizontal spectra recorded on the foundation or pillar (F, R, P sites in Figure 1) compared to the real free-field conditions (site S in Figure 1) under microtremors is expected and effectively measured. This effect can easily be observed by taking two short measurements one on the foundation/pillar and one on the natural soil just around the foundation, as we are going to show.

Phenomenological evidence

We consider the ALF and MRN seismic stations (Figure 1) and compare the spectra of the recordings taken on the pillar (P), on the foundation (F), on the foundation rim (R) and on the natural soil just outside the station (S), at the same time (Figure 8). We clearly see that while moving from the foundation center to its rim, to the natural soil, the amplitude of the horizontal spectra significantly increases. The effect is clear from 4 Hz and 10 Hz upwards, for ALF and MRN respectively, and essentially depends on the foundation width, more than on its thickness (Castellaro and Mulargia, 2009). Again, there is no significant difference between the motion acquired on the pillars – just theoretically but not effectively isolated from the rest of the foundation – and the motion on the foundation. They both severely alter the recorded motion, compared to the soil one, of a factor up to 10 times in amplitude.

In Figure 8 (gray arrows) we clearly see that the F, P, R spectra are also severely affected by the natural frequencies of the housings (4 Hz for ALF and the already mentioned 10 Hz for MRN).

The foundation effect (decay in the horizontal spectral components) and the housing effect (peaks of increased amplitude in the horizontal components at the eigen-frequencies of the housing) overlap and are both present in the foundation (F) and pillar (P) recordings.

This issue is not typical only of foundations on soft soils. Outcropping rock is often weathered or detensioned, as it occurs in tunnels, and this results in an impedance contrast between the rock and the foundation, too. In Figure 9 we present the H/V curves acquired on a seismic station in Bulgaria (Sofia) installed inside a tunnel in rock (granite). The acquisition performed on the rock shows a flat H/V with amplitude equal to 1, as expected. The acquisition performed on the concrete platform constructed to host a number of instruments on the rock, shows a significantly deamplified H/V ratio from 7 Hz upwards, due to the deamplification of the horizontal components.

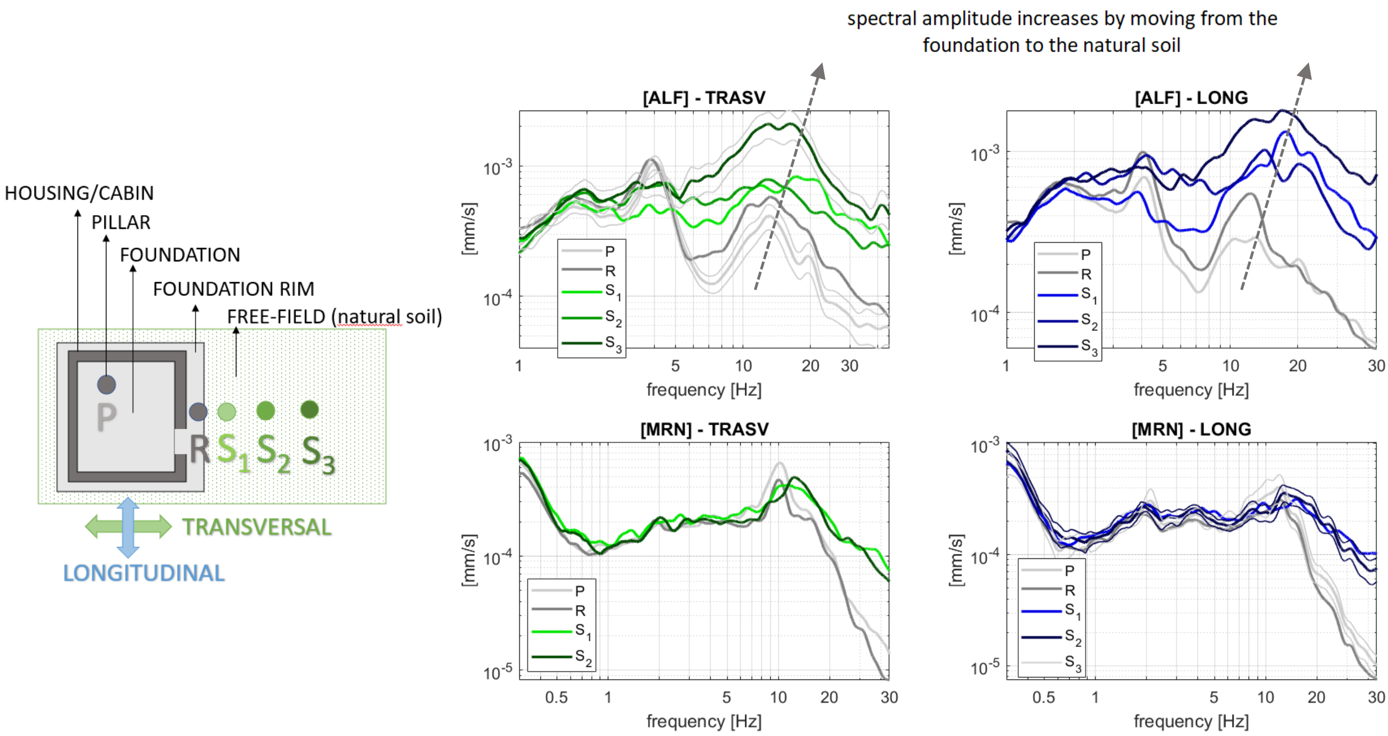

Figure 8. Velocity spectra recorded at different sites at the ALF and MRN sites, by moving from the pillar to the foundation to the surrounding soil. The typical distance between P and S3 is less than 10 m. Both the housing effect (peaks at 4 Hz for ALF, at 10 Hz for MRN) and the foundation effect (deamplification of the horizontal components of motion at P and R compared to the soil sites S) are visible. The standard deviation of the spectra is shown only in some extreme cases, not to impair the readability of the plots. Its amplitude is approximately the same also when not shown.

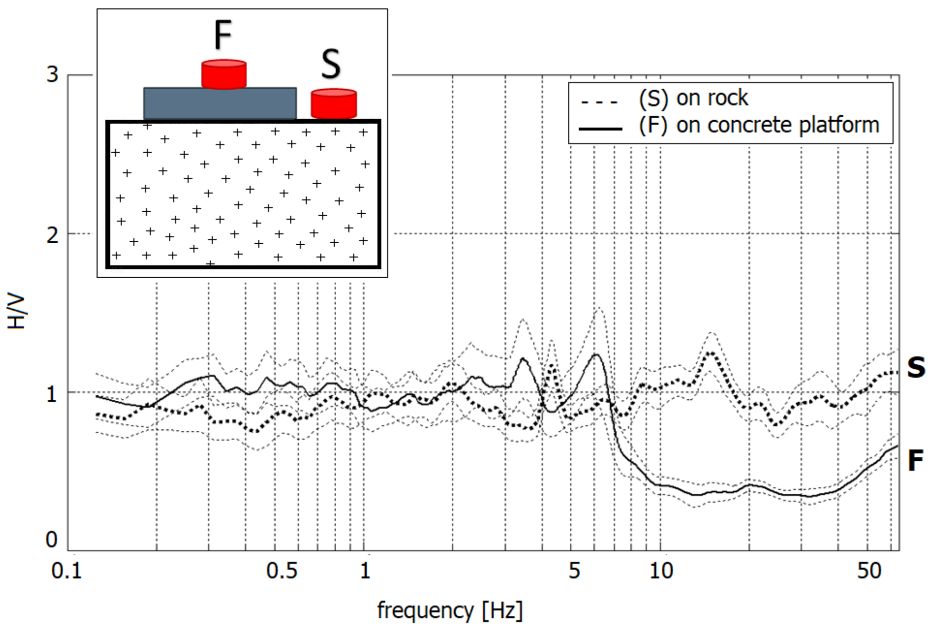

Figure 9. Microtremor H/V ratio recorded on a granite rock (dashed line) and on a concrete slab on the rock (black line). The concrete platform, being stiffer than the rock, produces a deamplified H/V curve at frequencies larger than 7 Hz.

Numerical evidence

By using the FE numerical tools Ansys Academy 2020R1, we modelled a square concrete foundation slab (ρ = 2400 kg/m^3, E = 30 GPa, size 4 * 4 m^2, 0.5 m thick) immersed in a soil (ρ = 2000 kg/m^3, μ = 20 MPa; Vs = 100 m/s). The mesh size was refined close to the slab, where we were interested in a better definition and was coarser while moving away from the slab, to reduce the computation time. We input an impulsive motion with horizontal direction on one side of the model (star in Figure 10a) that gives birth to surface waves propagating and reaching the foundation slab, which is put into oscillation (Figure 10b). The reason for the choice of an impulsive motion is that it is the ideal excitation, virtually containing the whole frequency spectrum with the same amplitude (white noise).

The displacement amplitude spectrum recorded at the centre and on the top of the slab (red dot in Figure 10) is compared with the spectrum recorded at the same place but in the case of no foundation. A clear deamplification of the motion on the slab can be seen from 20 Hz upwards (Figure 10c), which stands for a deamplification at wavelengths lower than 10 m (which is twice the slab size, Figure 10d). This is what we basically found experimentally with surface waves.

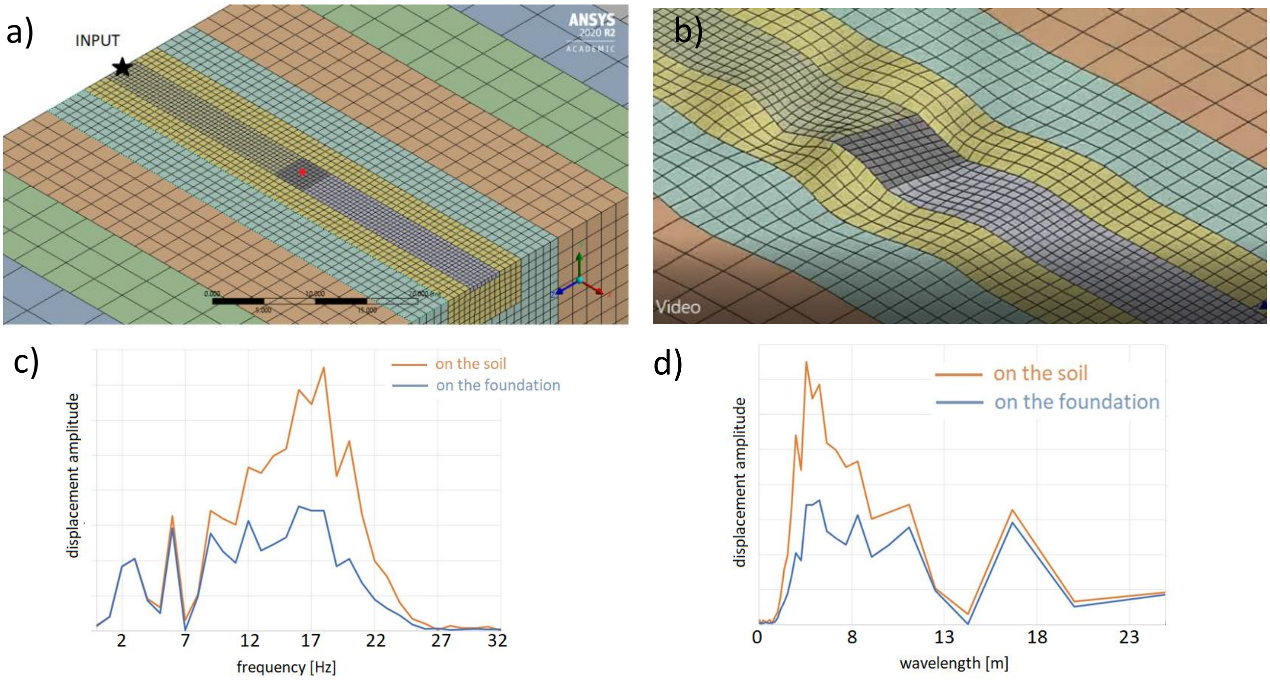

*Figure 10. a) FE model of a slab (gray central square, 4*4 m²) immersed in a soft soil. The different colors indicate the volumes with meshes of different size. The underlying subsoil properties are uniform; b) the slab hit by surface waves generated by an input applied at the star location of panel a); c) displacement spectra of the motion recorded at the centre and on the top of the slab and the motion in case of no slab; d) as panel c) but in terms of wavelengths.*

Other possible consequences

The deamplification of the horizontal components (H) due to a stiff foundation might sometime lead to the wrong conclusion that the dominant component of motion during an earthquake is the vertical one (V). By analyzing 123 response spectra of motion recorded at 41 alluvial sites, Bozorgnia *et al.* (1995) noted that the H/V spectral ratios of motion were well below the assumed 1 to 2/3 value at frequencies larger than 6-10 Hz. This is reported to be common in the near field (Chopra, 1966), but this could also be partly or fully explained by the fact that near earthquakes are rich in high frequencies and that seismic installations – particularly those settled on soft soils – modify the seismic input at high frequency, specifically decreasing its H/V ratio.

Luzi *et al.* (2013) observed that, during the May 20th 2012 Mw 5.9 earthquake, the closest-to-the-epicentre MRN station recorded a vertical acceleration larger than the horizontal ones (Figure 11). A number of authors mentioned this as one of the reasons for many of the observed collapses (Vannucchi *et al.,* 2012; Romeo, 2012; Ercolino *et al.*, 2012; Andreini *et al.*, 2014; Decanini *et al.*, 2012; Carydis *et al.*, 2012). It is true that the Peak Ground Acceleration (PGA) recorded by the MRN station occurred in the vertical component (Figure 11 top line), but the earthquake spectra (Figure 11 bottom line) show that the vertical component was larger than the horizontal ones only at frequencies larger than $\simeq$10 Hz.

This very same pattern (H/V < 1 at f > 10 Hz) is visible in the microtremor H/V spectra collected on the station pillar but it is no more visible in the recordings collected at just 2 m distance from the station, in real free-field conditions (Figure 12). We thus propose that in the case of this earthquake the dominant vertical component of PGA was possibly not a real feature of the earthquake, but once more an artifact induced by the foundation around the seismic sensor, that strongly deamplified the high frequency horizontal components.

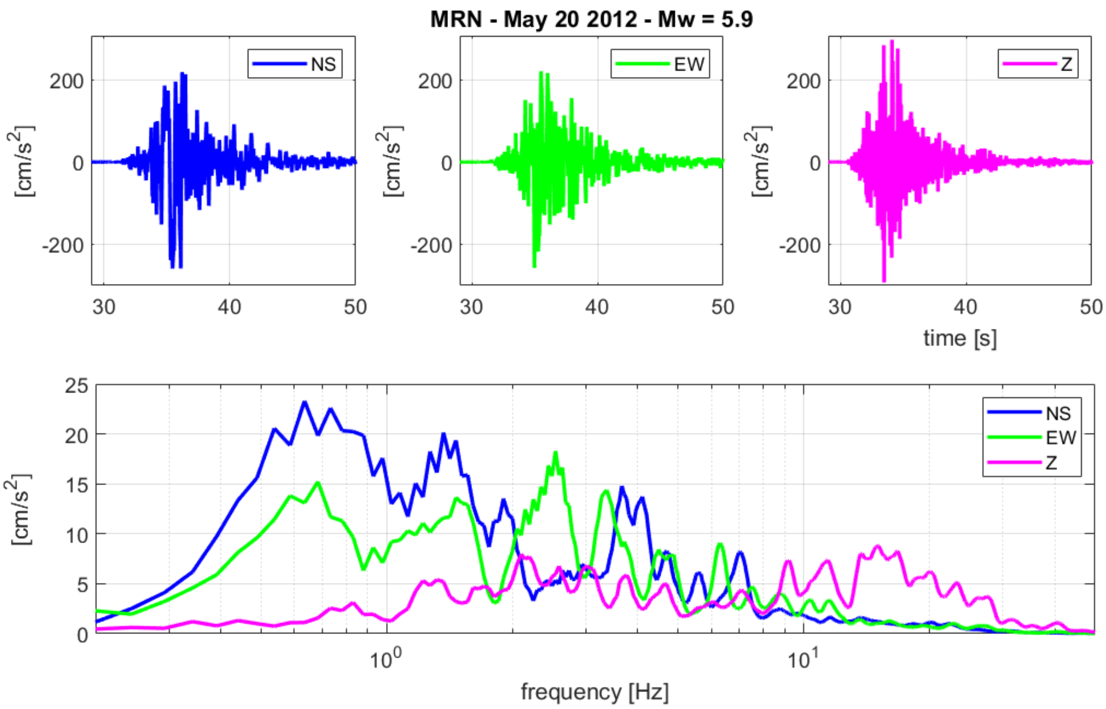

Figure 11. 3C recordings of the Mirandola May 20th 2012 earthquake recorded at the MRN station. Top: time series. Bottom: acceleration amplitude spectra.

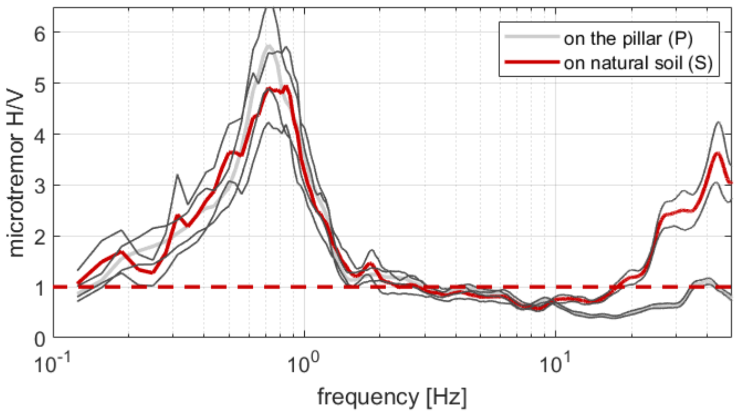

Figure 12. Microtremor H/V ratios recorded at the MRN station on the pillar (P) and in free-field (S). The average value is marked by the thick line, standard deviation is represented by the thin lines. The foundation effect is clear at frequencies larger than 10 Hz.

The pillar effect

As anticipated, the intention of letting the seismometers be independent from the surrounding housings led to the cut of the foundations and to the construction of pillars, directly set into the ground in the middle or on the corner of foundations (Figure 1, MRN in Figure 2). Pillars are typically cylinders of 0.6 m diameter and 1.5 m height, set into the ground for at least 0.5 m. As seen, this cut is not much effective because the structure and the pillar are rooted on the same soil and the transmission of the reciprocal motion is warranted by the soil itself.

Another potential problem emerges. Also pillars have their own vibration modes that are certainly recorded by the sensor applied on their top. Do these modes occur at frequencies of engineering interest? Concrete pillars typically installed in seismic stations are ‘beams’ dominated by shear, rather than flexural deformation and their eigen-modes are expected to occur at several tens of hertz, well beyond the range of interest in engineering seismology.

The eigen-frequency of a shear beam with a fixed constraint can be computed analytically. However, in the presence of an earthquake excitation the soil should be considered as an elastic body and a numerical investigation is more suitable. By using again the FE numerical tools Ansys Academy 2020R1, we modelled a pillar with the dimensions given above, density $\rho = 2.4 \cdot 10^3\ kg/m^3$, Young modulus $E = 30\ GPa$, stuck for 0.5 m into a soil with $\rho = 2 \cdot\ 10^3\ kg/m^3, E = 45\ MPa, V_S = 150\ m/s$ (Figure 13). By applying an impulse in horizontal direction with $V_0 = 1\ m/s$ and observing the free oscillations, we found that the eigen-frequency of the pillar is 28 Hz. This is hard to measure in real cases because the pillars are thick and the displacement under microtremor very weak, however we can expect that on average this kind of pillars vibrates at frequencies around 30 Hz and this value increases if, e.g., they are stuck at shallower depth.

It can be expected that the pillar moves independently from the foundation during an earthquake. However, the reduction in the horizontal components due to the foundation effect on surface waves still exist, as well as the transmission of the housing eigen-modes through the soil, as we have shown in the previous examples.

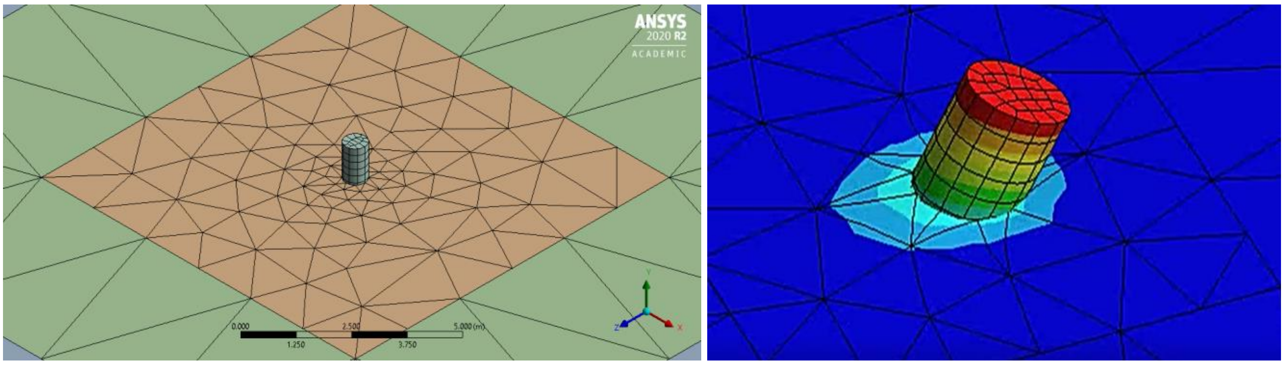

Figure 13. FE model of a homogenous pillar stuck into a soft soil.

Diffusion and identification of the problem

We estimated that as of 2021, in Italy, at least 35% of the ≃600 accelerometric IT stations are hosted inside 4-5 m side, 7-9 m height towers of the electrical national service (Figure 14). A further 3% are hosted in other types of buildings and 18% inside minihouses, that is structures like the MRN case we discussed. Most of them is also settled on soft soils (C, D, E categories according to EC8), where soil-structure interaction is expected to be large. We thus expect that the aforementioned issues affect at least half of the accelerometric

IT Italian network (clearly with different severity according to the specific conditions), but this is certainly not an issue restricted to Italy (see also Hollender *et al.*, 2020).

We propose a simple way to identify the existence of a potential installation-induced problem and assess the range of fidelity of the response of a seismic station to the ground motion. The approach is based on the following actions:

1) take a recording on the top of the seismic cabin (T) to identify its natural frequency,
2) take a set of simultaneous recordings on the pillar (P), on the foundation (F) and under truly free-field conditions (S). We are aware that at some sites a 'truly free-field' condition cannot even be achieved. We also warn that 'simultaneous' here means just at the same time but with no need for a real synchronization of all instruments, as no phase but only amplitude spectra are analyzed,
3) compare T and P (or T and F) spectra: these will immediately reveal the degree of rocking of the housing and tell what fraction of the housing motion is radiated to the foundation under weak motion,
4) compute the F/S or P/S spectral ratios. This will reveal to what extent the sensors placed on the foundation/pillar record a deamplified horizontal motion compared to the real free-field conditions and in what frequency interval. Expect that the larger the foundation size, and the softer the soil compared to the foundation, the larger the frequency interval affected by these issues.

We warn that the recordings to assess the structure eigen-frequencies (item 1) should be done along the structural main axes, but these may not coincide with the NS-EW axes of the seismometer/accelerometer installed inside the structure. In this case, *ad hoc* axis rotations should be performed. We also warn that in order to perform the comparisons above, some spectral smoothing in mandatory but this should not exceed a few percent of the central frequency otherwise the spectral peaks due to the housing eigenmodes will appear less clear.

The proposed approach is based on our experience with ambient noise recordings. The seismic installation impact during earthquake motion can be different and is certainly more difficult to be predicted because it depends on a number of additional factors (earthquake directivity, depth, size etc.).

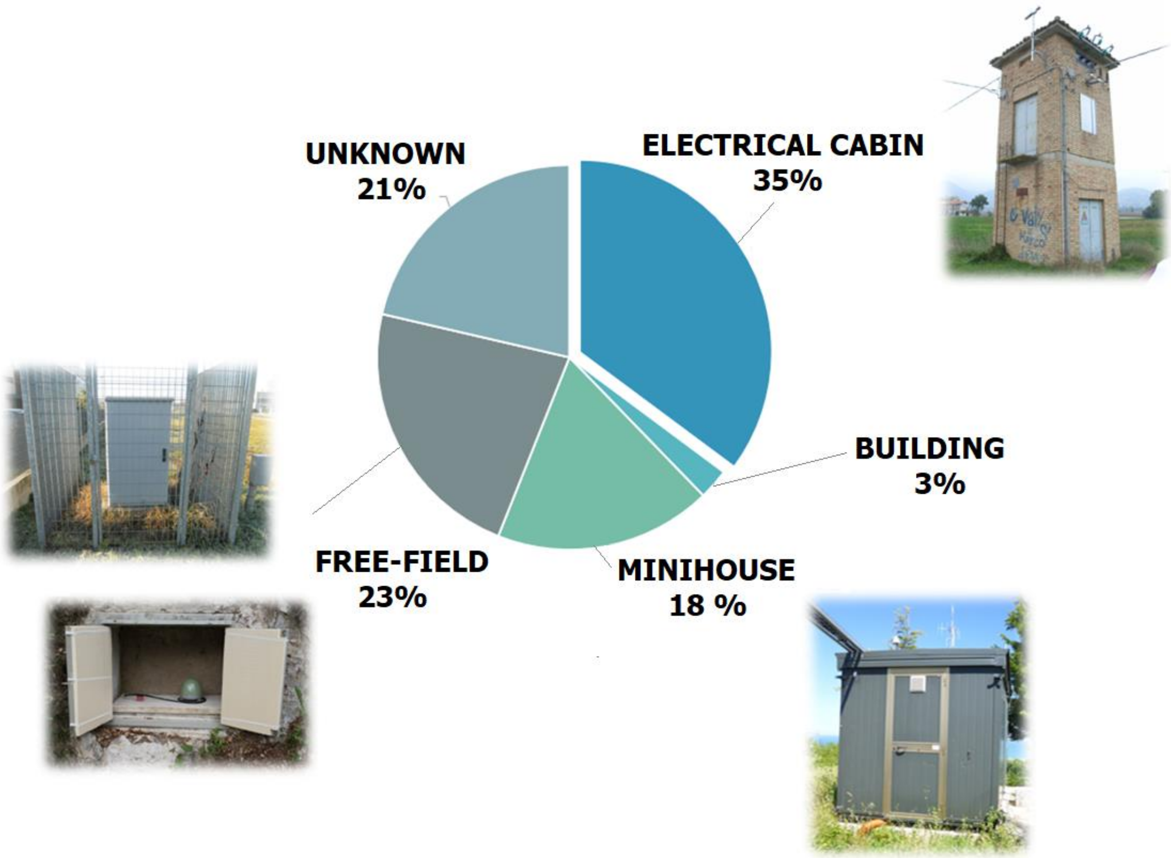

Figure 14. Percentage of the seismic installations of the Italian accelerometric network, as of 2021.

Discussion and Conclusions

Bormann *et al.* (2002, chapter 7) wrote that seismic site selection is not often given the amount of study it requires. Maybe also the hosting structure is not given the consideration it requires (Hollender *et al.*, 2020) as the design and construction of seismic stations has not much evolved over time.

The presence of a structure around an instrument perturbs the recorded motion in a way that can be summarized in three effects.

The first one is the transmission of the structure own motion to the foundation and the surrounding ground. Sensors placed inside the structure record, therefore, a composite signal, made of seismic waves and of the response of the structure to them. We showed that cutting the foundation around the sensor pillars gives no benefits in isolating the sensor from the housing motion, as the vibrations are transmitted very efficiently through the common soil.

The second effect is that a foundation, typically made of reinforced concrete, acts as a layer with seismic impedance much higher than any natural soil. Surface waves striking an extended rigid layer like a foundation, will be mostly reflected backwards as they hit the foundation. They will shake the structure, but only a small fraction of them will cross the foundation and will be recorded by the instruments installed on the foundation. Foundations violate the principle of physical measurements according to which when an interface is needed between an instrument and the object of measurement (the ground) then the interface must have an impedance as close as possible to the object of measurement, to minimize the perturbation of the wavefield. Concrete slabs/pillars do not have this property, not even always when installed on very stiff rock.

As a consequence, in seismic tremor recordings carried out inside a structure, a fraction of waves is missing. The numerical and experimental evidence on earthquake data is not so clear in terms of deamplification. Luco *et al.* (1990) and Hollender *et al.* (2020) documented more often the opposite effect, that is of amplification at frequencies larger than 10 Hz. However, in both cases (ambient noise and earthquakes) the seismic motion is strongly altered by the presence of the foundation.

The third issue is related to the pillar that can alter the recorded motion by means of its own eigenmodes. This effect, however, is mostly confined to frequencies beyond the range of engineering interest.

We noted that particularly the first problem can affect even the modern fibre-glass installations since their smaller mass and stiffness combination turns into natural frequencies of vibration still falling within the range of engineering interest. Fiber-glass cabins are also often hosted on large concrete slabs where other instruments (typically meteorological) are installed. This makes the frequency interval, where deamplification of horizontal motion recorded by the seismometer is measured, wider.

Installing seismic stations inside structures does not affect the earthquake magnitude estimates, that are usually performed at very long periods and does not affect the hypocentral estimates, which are based on the arrival times of specific waves.

However, even by excluding the installations inside proper buildings, the soil-structure interaction at the seismic stations placed on surface can, in our experience, produce artefactual patterns at least down to 2 Hz, (this depends on the size and properties of the housing). The influence of the cabin self-modes on the recordings also leads to artefactual spikes in the response spectra typically on the plateau. The opposite (a reduction in the response spectra) effect is expected because of the velocity inversion induced by the foundation.

Besides the fact that these two effects can partly compensate in the response spectra, an issue remains about the reliability of the motion recorded from the seismic stations at high frequency. The strong-motion/accelerometric sensors and the short-period seismometers, which are dedicated to the detection of the mid-to-high-frequency motion, are thus those most affected by the seismic installation. This has consequences in the assessment of the station H/V curves, of seismic site effects in terms of PGA, on the computation of attenuation laws and ground motion prediction equations but probably also on the often observed unexpected large vertical motion compared to the horizontal one during earthquakes.

In conclusion, we believe that besides the parameters (Vs30, soil classes etc.) that start to be routinely introduced in the seismic archives, assessing the maximum reliable frequency f_{max} of earthquake and microtremor recordings (under which no soil-structure interaction is expected) is a mandatory step. To this aim, it should also be reminded that due to the possible non-elastic behavior under strong motion, such f_{max} established under weak motion could even be overestimated. This is because the eigen-frequencies of structures under strong-motion can be lower than under ambient noise excitation again due to the soil-structure interaction. We provided a simple scheme to assess this maximum reliable frequency f_{max}.

As a very final 'detail', we observe that seismometer/accelerometers also have natural frequencies, meant as resonances of the instrumental case. Accelerometers are usually smaller and screwed to the pillars, which makes the natural frequencies of their boxes (and content) shift to very large values. On the opposite, when dealing with bulky long-period seismometers, the natural frequency of their case (and content) can be in the range of few tens of hertz. This also depends on the instrument-to-soil/pillar/foundation coupling. In some extreme cases, particularly with temporary installations, also this point could be considered because it can lead to artefactual amplification of the recorded motion above 10 Hz.

Data and Resources

The data collected at the seismic station installations were collected by the authors and by those mentioned in the acknowledgments. The accelerometric records used in this paper were provided by ITACA (D'Amico *et al.*, 2020), INGV Itaca, last accessed Jan. 2022.

Declaration of Competing Interests

The authors acknowledge there are no conflicts of interest recorded.

Acknowledgments

We thank Giovanni Lattanzi for Figure 1, Martina Delvecchio and Anna Ferrara for the computations used to build Figure 14, Antonella Gorini from Dipartimento della Protezione Civile for providing access to the MRN station and the two workers from ENEL who assisted us during the measurements. We thank Stefano Isani for the continuous support in terms of structure dynamics. We thank Alfredo Pitullo and the Consorzio per la Bonifica della Capitanata (Contratto di Consulenza Commissionata tra Consorzio per la Bonifica della Capitanata e Dipartimento di Fisica e Astronomia dell'Alma Mater Studiorum – Università di Bologna 2019-2021) for funding some of the presented surveys. We thank Umberto Borgia, Luigi Perricone and Riccardo Panzeri for their help, in 2014, in collecting many of the measurements here presented, in the frame of the

DPC-INGV-S2-2014 Project “Constraining Observations into Seismic Hazard”, which is here acknowledged, too. Long time has passed since then, but the memory of those days is still alive. Thank you.

References

Andreini, M., A. De Falco, L. Giresini L., M. Sassu (2014). Structural damage in the cities of Reggiolo and Carpi after the earthquake on May 2012 in Emilia Romagna*, Bull. Earthquake Eng.* **12** 2445-2480.

Bormann, P. (2012). New Manual of Seismological Observatory Practice (NMSOP-2), Potsdam: Deutsches GeoForschungszentrum GFZ, IASPEI.

Bozorgnia, Y., M. Niazi, K.W. Cambell (1995). Characteristics of Free-Field Vertical Ground Motion during the Northridge Earthquake, *Earth. Spectra* **11** 515-525.

Bycroft, G.N. (1978). Soil-structure interaction at higher frequency factors, *Earthq. Eng. Struct. Dyn.* **5** 235-248.

Bycroft, G.N. (1980). Soil-foundation interaction and differential ground motions, *Earthq. Eng. Struct. Dyn.* **8** 235-248.

Castellaro, S. (2016a). Soil and structure damping from single station measurements, *Soil Dyn. Earthq. Eng.* **90** 480-493.

Castellaro, S. (2016b). The complementarity of H/V and dispersion curves, *Gephysics* **81** T323-T338.

Castellaro, S., F. Mulargia (2009). The effect of velocity inversions on H/V, *Pure and Applied Geophysics* **166** 567-592.

Castellaro, S., F. Mulargia (2010). How far from a building starts the tremor free-field? The case of three most famous Italian towers and of a modern building, *Bull. Seism. Soc. Am.* **100** 2080-2094.

Castellaro, S., L.A. Padron, F. Mulargia (2013). The different response of apparently identical structures: a far-filed lesson from the Mirandola 20th May 2012 earthquake, *Bull. Earthq. Eng.*, **12**, 2481-2493.

Cavalieri, F., A.A. Correia, R. Pinho, (2021). Variations between foundation-level recordings and free-field earthquake ground motions: numerical study at soft-soil sites, *Soil Dynamics and Earthquake Engineering* **141** 106511.

Carydis, P., C. Castiglioni, E. Lekkas, I. Kostaki, N. Lebesis, A. Drei (2012). The Emilia Romagna, May 2012 earthquake sequence. The influence of the vertical earthquake component and related geoscientific and engineering aspects, *Ingegneria Sismica* **2-3**, 31-58.

Chavez-Garcia, F.J., M. Cardenas-Soto (2002). The contribution of the built environment to the free-field ground motion in Mexico City, *Soil Dyn. Earthq. Eng.* **22** 773–780.

Chopra, A.K. (1966). The importance of the vertical component of earthquake motions, *Bull. Seism. Soc. Am.* **56** 1163-1175.

Clough, R.W., J. Penzien (1975). *Dynamics of structures*, Mc-Graw Hill.

Clouteau, D., D. Aubry (2001). Modifications of the ground motion in dense urban areas, *J. Computational Acoustics* **9** 1659-1675.

Cornou, C., P. Guéguen, P.-Y. Bard, E. Haghshenas (2004). Ambient noise energy bursts observation and modeling: Trapping of harmonic structure-soil induced–waves in a topmost sedimentary layer, *J. Seismol.* **8** 507–524.

Crouse, C.B., B. Husmand (1989). Soil-structure interaction at CDMG and USGS accelerograph stations, *Bull. Seismol. Soc. Am.* **79** 1–14.

Cultrera, G., C. Cornou, G. Di Giulio, P.-Y. Bard (2021). Indicators for site characterization at seismic station: recommendation from a dedicated survey, *Bull. Earthquake Eng.* **19** 4171–4195

D'Amico, M.C., C. Felicetta, E. Russo, S. Sgobba, G. Lanzano, F. Pacor, L. Luzi (2020). ITalian ACcelerometric Archive (ITACA), version 3.1, Istituto Nazionale di Geofisica e Vulcanologia (INGV).

Decanini, L.D., D. Liberatore, L. Liberatore, L. Sorrentino (2012). Preliminary Report on the 2012, May 20, Emilia Earthquake, v.1, http://www.eqclearinghouse.org/2012-05-20-italy-it/

Ditommaso, R., M.R. Gallipoli, M. Mucciarelli, F.C. Ponzo (2010a). Effect of a single vibrating building on free-field ground motion: numerical and experimental evidences*, Bulletin of Earthquake Engineering* **8** DOI: 10.1007/s10518-009-9134-5.

Ditommaso, R., S. Parolai, M. Mucciarelli, S. Eggert, M. Sobiesiak, J. Zschau (2010b). Monitoring the response and the back-radiated energy of a building subjected to ambient vibration and impulsive action: the Falkenhof Tower (Potsdam, Germany), *Bulletin of Earthquake Engineering* **8** DOI: 10.1007/s10518-009-9151-4.

Ercolino, M., G- Magliulio, G. Manfredi (2016). *The lesson learnt after Emilia-Romagna earthquakes on precast RC structures: a case-study,* 1st International Conference on Natural Hazards & Infrastructure 28-30 June, Chania, Greece.

Guéguen, P., P.-Y. Bard, C.S. Oliveira (2000). Experimental and numerical analysis of soil motion caused by free vibration of a building model, *Bull. Seism. Soc. Am.* **90** 1464-1479.

Guéguen, P., P.-Y. Bard, F.J. Chavez-Garcia (2002). Site-city seismic interaction in Mexico Citylike environments: An analytic study, *Bull. Seism. Soc. Am.* **92** 794- 811.

Guéguen, P., P.-Y. Bard (2005). Soil-structure and soil-structure-soil interaction: experimental evidence at the Volvi test site, *J. Earthq. Eng.*, **9**, 657–693.

Hollender, F., Z. Roumelioti, E. Maufroy, P. Traversa, A. Mariscal (2020). Can we trust high-frequency content in strong-motion database signals? Impact of housing, coupling, and installation depth of seismic sensors, *Seismological Research Letters* **91** 2192-2205.

Isbiliroglu, Y., R. Taborda, J. Bielak, (2015). Coupled Soil-Structure Interaction Effects of Building Clusters during Earthquakes, *Earthq. Spectra* **31** 463-500.

Jennings, P.C. (1970). Distant motion from a building vibration test, *Bull. Seism. Soc. Am.* **60** 2037-2043.

Kham, M., J.-F. Semblat, P.-Y. Bard, P. Dangla. (2006). Seismic site–city interaction: main governing phenomena through simplified numerical models, *Bull. Seism. Soc. Am.* **96** 1934-1951.

Kumar N., J.P. Narayan, 2018. Quantification of site–city interaction effects on the response of structure under double resonance condition, *Geophysical Journal International* **212** 422–441.

Laurenzano, G., E. Priolo, M.R. Gallipoli, M. Mucciarelli, F.C. Ponzo (2010). Effect of vibrating buildings on free-field motion and on adjacent structures: the Bonefro (Italy) case history, *Bull. Seism. Soc. Am.* **100** 802-818.

Luco, J.E., J.G. Anderson, M. Georgevich (1990). Soil-structure interaction effects on strong motion accelerograms recorded on instrument shelters, *Earthq. Eng. Struct. Dyn.* **19** 119-131.

Luco, J., H.L. Wong (1986). Response of a rigid foundation to a spatially random ground motion, *Earthq. Eng. Struct. Dyn.* **14** 891-908.

Luzi, L., F. Pacor, G. Ameri, R. Puglia, P. Burrato, M. Massa, P. Augliera, G. Franceschina, S. Lovati, R. Castro (2013). Overview on the Strong-Motion Data Recorded during the May–June 2012 Emilia Seismic Sequence, *Seismological Research Letters*, **84** 629-644.

Massa, M., S. Marzorati, C. Ladina, S. Lovati (2010). Urban seismic stations: soil-structure interaction assessment by spectral ratio analyses, *Bull. Earthquake Eng.* **8** 723–738.

Mucciarelli, M., M.R. Gallipoli, F.C. Ponzo, M. Dolce (2003). Seismic waves generated by oscillating building, *Soil Dyn. Earthq. Eng.* **23** 255-262.

Romeo, R. (2012). Emilia (Italy) M5.9 earthquake on 20 May 2012: an unusual pattern of liquefaction*, Italian J. Eng. Geol. Environ.* **2** 75-84.

Şafak, E. (1998), New approach to analyzing soil-building systems, *Soil Dyn.and Earthq. Engin.* **17** 509-517.

Schwan, L., C. Boutin, L.A. Padron, M.S. Dietz, P.-Y. Bard, C. Taylor (2016). Seismology Site-city interaction: theoretical, numerical and experimental crossed-analysis, *Geophys. J. Int.* **205** 1006–1031.

SESAME (2004). Guidelines for the implementation of the H/V spectral ratio technique on ambient vibrations: Measurements, processing and interpretation, SESAME European Research Project WP12, deliverable no. D23.12.

Vannucchi, G., T. Crespellani, J. Facciorusso, A. Ghinelli, C. Madiai, A. Puliti, S. Renzi (2012). Soil liquefaction phenomena observed in recent seismic events in Emilia-Romagna Region, Italy, *Ingegneria Sismica* **2-3** 20-29.

Wirgin, A., P.-Y. Bard (1996). Effects of building on the duration and amplitude of ground motion in Mexico City, *Bull. Seism. Soc. Am.* **86** 914-920.

Wong, H.L., M.D. Trifunac (1975). Two dimensional antiplane building-soil-building interaction for two or more buildings and for incident plane SH waves, *Bull. Seismol. Soc. Am.* **65** 1863-1865.

Zoepprtiz, K. (1919). On reflection and propagation of seismic waves**,** *Gottinger Nachrichten* **1** 66-84.

Silvia Castellaro - Dipartimento di Fisica e Astronomia, Alma Mater Studiorum Università di Bologna, viale C. B. Pichat 8, 40127 Bologna Italy, silvia.castellaro@unibo.it

Giulia Alessandrini - Dipartimento di Fisica e Astronomia, Alma Mater Studiorum Università di Bologna, viale C. B. Pichat 8, 40127 Bologna Italy, giulia.alessandrin11@unibo.it

Giuseppe Musinu - ENSER srl, viale A. Baccarini 29, 48018 Faenza, Ravenna – Italy, giuseppe.musinu@enser.it

List of figure captions

Figure 1. Schematic illustration of a typical seismic installation inside a small structure with a direct foundation. T (top) is the measurement point on the top of the structure (to characterize its fundamental mode), P on the pillar, F on the foundation, R on the foundation rim and S on natural soil.

Figure 2. A set of stations of the Italian accelerometric (IT) and seismic (IV) network: small housing (MRN), tower-structures of the national electric service (FRN, NAS, CRL, PNN, ALF) and fiber-glass cabin (CER). A typical pillar with the cut separating it from the foundation is also shown for the MRN station. The pillar is present in most of the Italian installations and can also be square in shape, as in the case of CER. The instruments used for this survey can be seen in the panel of MRN and CER (blue and red boxes). The letter P stands for pillar, F for foundation, R for foundation rim.

Figure 3. Spectral ratios of the motion recorded along the transversal direction of the cabin MRN at different locations, whose symbols are given in the right panel. The T/S_{ref} and T/F spectral ratios show the natural vibration modes of the structure (gray arrows at 10 Hz, 17 Hz). The P/S_{ref} and F/S_{ref} ratios show the effect of the foundation on the incoming waves in respect to the real free-field condition. If the foundation induced no effect, these ratios should be equal 1 at all frequencies. S_1/S_{ref} is the ratio between the recording acquired on the soil just off the station (S_1) and on the soil at a few meters distance from the station (usually 3-5 m from the foundation rim). S_1/S_{ref} tends to 1 but the eigen-mode of the structure is still visible. The standard deviation of the spectral ratios is shown only in the two extreme cases, not to impair the readability of the plots. It was checked that its amplitude is in the same order of magnitude also when not shown.

Figure 4. Spectral ratios of the motion recorded along the transversal direction of the cabins NAS and PNN at different locations, whose symbols are given in the right panel of Figure 3. In the F/S_{ref} ratios the natural vibration modes of the structure (6.8 Hz and 5.2 Hz for NAS and PNN, respectively) can be clearly identified. These are progressively less noticeable in the S_1/S_{ref} and S_2/S_{ref} ratios. Thick lines are the average values, thin lines indicate the standard deviations.

Figure 5. Left panel: H/V curve computed on the data acquired from the official instrument installed on the pillar at the CRL station. According to the station report, 2 peaks pass the SESAME (2004) criteria. Our measurements (right panel), performed on the top of the cabin (T) and on the natural soil just off the station (S) clearly show that the 6 Hz peak is the eigen-period of the cabin and not a soil property. Thick lines are the average values, thin lines indicate the standard deviations.

Figure 6. Free-field earthquake records and response spectra (S, black) compared to those recorded on the top of a seismic station (T, red) and on the pillar inside the station (P, cyan). Panels a, b, c refers to the MRN station. Panels d, e, f to the FRN one. The average response spectra (thick lines) are obtained from 10 earthquakes (thin lines). Panels a, b, d, e show just one of the 10 selected earthquakes for each station, as an example.

Figure 7. Ambient noise recording acquired in (A) free-field conditions, (B) on the station pillar and response spectra in the two cases (C) for the MRN station. The input signal was 30 min long. Panel (A) an (B) show just a portion of it.

Figure 8. Velocity spectra recorded at different sites at the ALF and MRN sites, by moving from the pillar to the foundation to the surrounding soil. The typical distance between P and S3 is less than 10 m. Both the housing effect (peaks at 4 Hz for ALF, at 10 Hz for MRN) and the foundation effect (deamplification of the horizontal components of motion at P and R compared to the soil sites S) are visible. The standard deviation of the spectra is shown only in some extreme cases, not to impair the readability of the plots. Its amplitude is approximately the same also when not shown.

Figure 9. Microtremor H/V ratio recorded on a granite rock (dashed line) and on a concrete slab on the rock (black line). The concrete platform, being stiffer than the rock, produces a deamplified H/V curve at frequencies larger than 7 Hz.

Figure 15. a) FE model of a slab (gray central square, 4*4 m^2) immersed in a soft soil. The different colors indicate the volumes with meshes of different size. The underlying subsoil properties are uniform; b) the slab hit by surface waves generated by an input applied at the star location of panel a); c) displacement spectra of the motion recorded at the centre and on the top of the slab and the motion in case of no slab; d) as panel c) but in terms of wavelengths.

Figure 11. 3C recordings of the Mirandola May 20th 2012 earthquake recorded at the MRN station. Top: time series. Bottom: acceleration amplitude spectra.

Figure 12. Microtremor H/V ratios recorded at the MRN station on the pillar (P) and in free-field (S). The average value is marked by the thick line, standard deviation is represented by the thin lines. The foundation effect is clear at frequencies larger than 10 Hz.

Figure 13. FE model of a homogenous pillar stuck into a soft soil.

Figure 14. Percentage of the seismic installations of the Italian accelerometric network, as of 2021.